# Increased magnetic damping of a single domain wall and adjacent magnetic domains detected by spin torque diode in a nanostripe

Steven Lequeux, Joao Sampaio, Paolo Bortolotti, Thibaut Devolder, Rie Matsumoto, Kay Yakushiji, Hitoshi Kubota, Akio Fukushima, Shinji Yuasa, Kazumasa Nishimura, Yoshinori Nagamine, Koji Tsunekawa, Vincent Cros, and Julie Grollier

---

### Articles you may be interested in

Time-domain analysis of spin-torque induced switching paths in nanoscale CoFeB/MgO/CoFeB magnetic tunnel junction devices
J. Appl. Phys. **116**, 243902 (2014); 10.1063/1.4905023

Optically induced spin wave dynamics in [Co/Pd]8 antidot lattices with perpendicular magnetic anisotropy
Appl. Phys. Lett. **105**, 162408 (2014); 10.1063/1.4898774

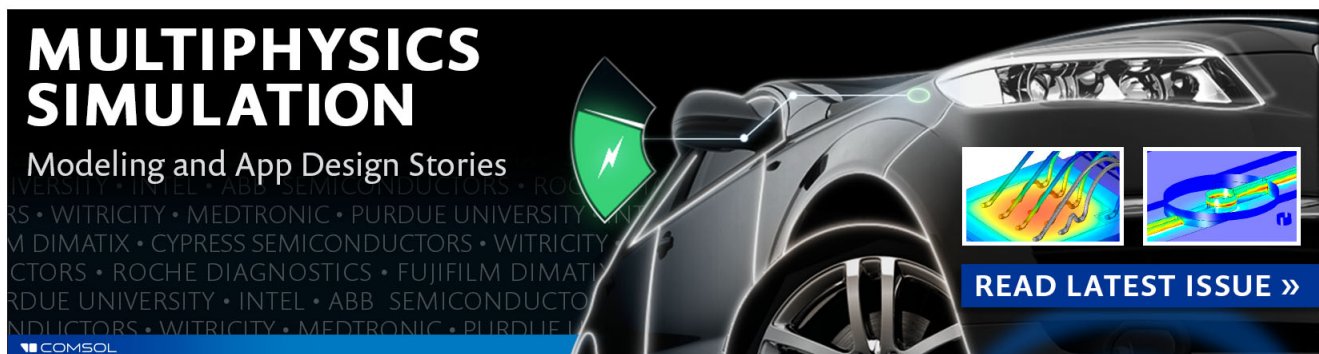Spin-wave excitations induced by spin current through a magnetic point contact with a confined domain wall
Appl. Phys. Lett. **101**, 092405 (2012); 10.1063/1.4745777

Current-induced motion of a transverse magnetic domain wall in the presence of spin Hall effect
Appl. Phys. Lett. **101**, 022405 (2012); 10.1063/1.4733674

Effect of electrical bias on spin transport across a magnetic domain wall
J. Appl. Phys. **96**, 7424 (2004); 10.1063/1.1815044

---

# Increased magnetic damping of a single domain wall and adjacent magnetic domains detected by spin torque diode in a nanostripe

Steven Lequeux,[1] Joao Sampaio,[1] Paolo Bortolotti,[1] Thibaut Devolder,[2] Rie Matsumoto,[3] Kay Yakushiji,[3] Hitoshi Kubota,[3] Akio Fukushima,[3] Shinji Yuasa,[3] Kazumasa Nishimura,[4] Yoshinori Nagamine,[4] Koji Tsunekawa,[4] Vincent Cros,[1] and Julie Grollier[1]

[1]*Unité Mixte de Physique CNRS/Thales and Université Paris-Sud 11, 1 Ave. A. Fresnel, 91767 Palaiseau, France*
[2]*Institut d'Electronique Fondamentale, Univ. Paris-Sud, CNRS UMR 8622, Bât. 220, 91405 Orsay Cedex, France*
[3]*National Institute of Advanced Industrial Science and Technology (AIST), 1-1-1 Umezono, Tsukuba, Ibaraki 305-8568, Japan*
[4]*Process Development Center, Canon ANELVA Corporation, Kurigi 2-5-1, Asao, Kawasaki, Kanagawa 215-8550, Japan*

Spin torque resonance has been used to simultaneously probe the dynamics of a magnetic domain wall and of magnetic domains in a nanostripe magnetic tunnel junction. Due to the large associated resistance variations, we are able to analyze quantitatively the resonant properties of these single nanoscale magnetic objects. In particular, we find that the magnetic damping of both the domains and the domain wall is doubled compared to the damping value of the host magnetic layer. We estimate the contributions to the damping arising from the dipolar couplings between the different layers in the junction and from the intralayer spin pumping effect, and find that they cannot explain the large damping enhancement that we observe. We conclude that the measured increased damping is intrinsic to large amplitudes excitations of spatially localized modes or solitons such as vibrating or propagating domain walls. © 2015 AIP Publishing LLC.
[http://dx.doi.org/10.1063/1.4935203]

The spin torque diode effect provides an efficient tool to access the resonant properties of sub-micrometer magneto-resistive structures.[1] In particular, contrary to conventional ferromagnetic resonance techniques, the sensitivity allows probing of the dynamics of individual magnetic solitons, such as vortices or domain walls (DWs), which are predicted as information vectors in next generation magnetic devices.[2–9] By injecting a microwave current through the stack at resonance, the spin torque can induce magnetization precession of the free layer. The magneto-resistance effect then converts this precession into resistance variations. These resistance oscillations, multiplied by the microwave current oscillating at the same frequency, give rise to a rectified dc voltage. Most spin torque diode studies have focused on the dynamical properties of uniform magnetization configurations,[10–14] although work has been also carried out on the vibration modes of magnetic solitons.[2–8] Moreover, previous work on DW were performed with metallic samples, where the magneto-resistance ratios are typically restricted to a few %. These low magneto-resistance ratios strongly limit the amplitude of the output dc signal. In the case of DW vibrations, generally confined and of limited amplitude, it is therefore very difficult to extract quantitative parameters other than the resonance frequency of the wall.[2–8]

In this letter, we take advantage of the large tunnel magneto-resistance (TMR) ratios provided by MgO-based magnetic tunnel junctions to probe the dynamics of a DW and its neighboring domains by the spin torque diode effect. The junction tracks were fabricated by electron beam lithography and ion beam milling from a film deposited by

magnetron sputtering with structure illustrated in Fig. 1(a), SiO$_2$//buffer/PtMn (15)/Co$_{70}$Fe$_{30}$ (2.5)/Ru (0.9)/CoFeB (3)/MgO (1.1)/Ni$_{80}$Fe$_{20}$ (5)/ Ru (10) (thicknesses in nanometers), and a TMR ratio of 30% (minimum resistance of 115 $\Omega$). A synthetic antiferromagnet (SAF), formed by the trilayer stack: Co$_{70}$Fe$_{30}$/Ru/CoFeB, prevents the formation of a domain wall in the CoFeB reference layer. The injection of a DW in the Ni$_{80}$Fe$_{20}$ free layer is facilitated by the arc shape geometry of our junctions, shown in Fig. 1(b). After the saturation of the free layer magnetization in the y direction with a strong external field (300 Oe, corresponding to a resistance of 130 $\Omega$), the DW is nucleated when the field is decreased below 75 Oe. In Fig. 1(c), micromagnetic simulations of the full stack performed using the OOMMF software[15] show that the DW is first nucleated in the center of the wire and is maintained at this position by the external field along the y direction. For small values of the applied field, the DW is shifted from the center of the arc to the right edge due to the noncompensated stray field of 5 Oe emitted by the reference layer. This behavior predicted by the micromagnetic simulations is in very good agreement with the experimental measurement of the junction resistance as a function of the decreasing field applied along the y direction, shown in Fig. 1(d). The bottom and top black dashed lines, given for reference, correspond to the resistance of the parallel (P) and anti-parallel (AP) states, respectively. Each change of the resistance value corresponds to a displacement of a DW in the Permalloy free layer. The first resistance plateau of 130 $\Omega$ for the field range between 75 and 26 Oe (blue square dot in Fig. 1(d)) corresponds to the magnetic
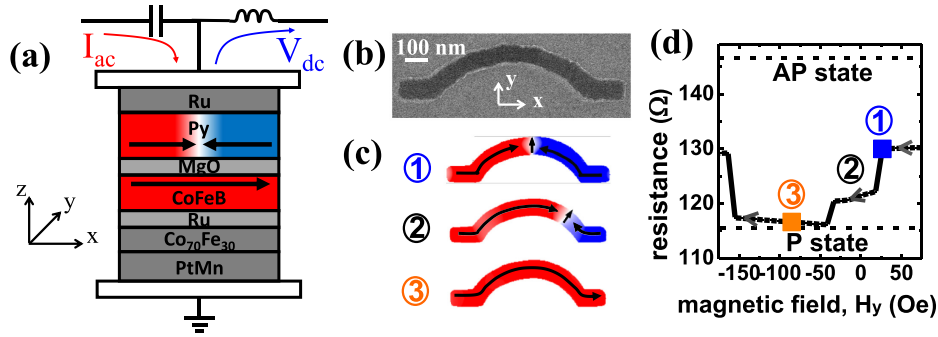
FIG. 1. (a) Schematic of the spin torque diode measurement set-up including the MgO-based magnetic tunnel junction with the DW in the Permalloy free layer. (b) Scanning electron microscope image of the sample. (c) Full-stack micromagnetic simulations representing the different steps in the DW displacement. (d) Resistance versus magnetic field measurements. Black dashed lines: resistance values of the P and AP states. Black line: evolution of the resistance when a DW is nucleated (e.g., blue square at 26 Oe) in the middle of the wire (1) then pinned in the right edge (2) until its expulsion (e.g., orange square at −85 Oe) (3).

configuration labeled 1 in Fig. 1(c). For lower fields, between 20 and −35 Oe, the DW shifts to a strong and reproducible pinning site due to the shape at the edge of the wire.[16] The resulting resistance plateau at 122 Ω in Fig. 1(d) corresponds to the magnetic configuration labeled 2 in Fig. 1(c). For negative fields larger than −40 Oe, the DW is expelled from the wire and the resistance value reaches the P state at 116 Ω (orange square dot labeled 3 in Fig. 1(d), and magnetic configuration labeled 3 in Fig. 1(c)).

We probe the resonant properties of our system via spin torque diode resonance in the configurations with and without a domain wall (respectively, blue square labeled 1 and orange square labeled 3 in Fig.1 (b)). We inject a microwave current $I_{hf}$ between the top and bottom electrodes, and sweep the frequency (see supplementary material[17]). We repeat this measurement for different values of applied field $H_y$. In the absence of dc current, the rectified voltage $V_{dc}$ has two main components[18]

$$V_{dc} = \frac{1}{2}\frac{\partial^2 V}{\partial I^2}\langle I_{hf}(t)^2 \rangle + \frac{\partial^2 V}{\partial I \partial q}\langle I_{hf}(t)q(t)\rangle. \quad (1)$$

The first term is a purely electrical background signal due to the bias dependence of the tunnel junction resistance, from which we extract the exact value of the injected microwave current in the junction. The second term is the spin torque diode contribution to the rectified voltage. It arises from the mixing between $I_{hf}$ and the resistance oscillations. Here, the resistance oscillations are induced through the TMR by the oscillations of the DW position in its potential well. The parameter q(t) represents the full time dependence of the position of the DW.

Figs. 2(a) and 2(b) show the rectified voltage response normalized by the square of the microwave current amplitude; $V_{dc}/I_{hf}^2$, at two different magnetic field values (see supplementary material[17]). Fig. 2(a) corresponds to a measurement at 26 Oe, performed at 130 Ω (state "1" in Fig. 1(d)), where the DW is positioned in the middle of the wire. Fig. 2(b) shows a measurement at −85 Oe, where the magnetization of the free layer has a quasi-uniform configuration corresponding to the parallel state (state "3" in Fig. 1(d)). The 26 Oe response curve shows two resonance signals at 1.24 GHz (mode 1) and 2.15 GHz (mode 2) while the −85 Oe response shows only one at 2.3 GHz (mode 2). We systematically observed two resonance signals in the field range

between 50 and −35 Oe where the DW is present, whereas only the higher frequency mode (mode 2) was observed between −40 and −150 Oe where the DW is expelled. The low frequency signal (mode 1) can therefore be ascribed to the DW oscillations while the higher frequency signal (mode 2) can be attributed to magnetization precession in the domains. When the DW is not present, the mode 2 is not strongly modified, only its resonance frequency is shifted by the external field applied to allow the DW expulsion. This means that the strongest vibrations responsible for the mode 2 are spatially located far enough from the DW so as not to be impacted by the DW vibrations when the DW is present.

Around the resonance frequency $f_0$, the normalized response curve takes the shape of a linear combination of Lorentzian and anti-Lorentzian profiles.[1,14] We fit the resonant signals of the mode 1 (DW) and 2 (domains) by the following expression (see supplementary material[17]):
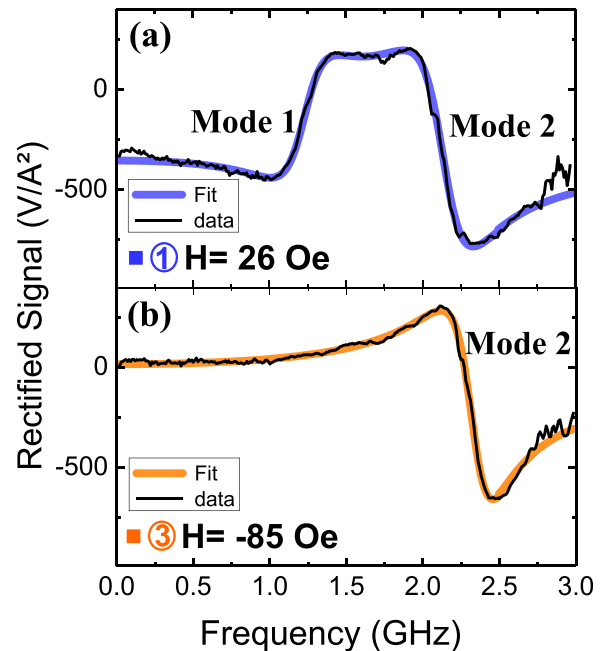


FIG. 2. Normalized rectified voltage $V_{dc}/I_{hf}^2$ as a function of frequency (a) Black line: measurement at 26 Oe with the DW positioned in the middle of the wire corresponding to a resistance of 130 Ω. Blue line: fit with Eq. (2). (b) Black line: measured at −85 Oe in the parallel state (DW expelled). Orange line: fit with Eq. (2).

$$\frac{V_{dc}}{I_{hf}^2} = \frac{A(f_0^2 - f^2) + Bf^2}{(f_0^2 - f^2)^2 + (\Delta f)^2} + C, \qquad (2)$$

where $f$ is the frequency of the microwave current $I_{hf}$ and the free parameters of the fit are the amplitudes A and B of the anti-Lorentzian and Lorentzian profiles, a constant shift C, the resonance frequency $f_0$, and the linewidth $\Delta$. The average value of $\Delta$ extracted from the measurements (Fig. 2) by fitting with Eq. (2) at different magnetic fields is about $0.4 \pm 0.02$ GHz both for mode 1 (DW) and mode 2 (domains). The magnetic damping parameter $\alpha$ is related to the linewidth.[11,12]

Here, in order to establish the correlation between $\Delta$ and the corresponding damping $\alpha$ for the DW and domains resonance signals, we perform micromagnetic simulations of only the 5 nm Py free layer at zero external field, the parameters of which are detailed in Ref. 19. In order to reconstruct the spin diode signal, we swept the frequency of a microwave current $I_{hf}$ between 0.9 and 3 GHz and extract the resulting magnetization oscillations. We plot, as a function of the frequency, the average amplitude of the product between the x component of the magnetization oscillations $M_x$ and $I_{hf} = I_0 \cdot \sin(2\pi ft + \phi)$ (Fig. 3). The $\phi$ parameter (respectively, equal to $\frac{\pi}{2}$ and 0 in Figs. 3(a) and 3(b)) is related to the resonant signal shape depending on the symmetry of the exciting force (Slonczewski or Field like torque[1]) and does not influence the linewidth. We find a resonant response for the DW and domains, respectively, at 1.7 (Fig. 3(a)) and 2.75 GHz (Fig. 3(b)), in good agreement with the experimental results (Fig. 2). For a damping parameter $\alpha = 0.01$, the linewidth extracted from the simulated spin diode signal by fitting with Eq. (2) is $0.15 \pm 0.002$ GHz both for modes 1 and 2 (Fig. 3).

For the particular case of the DW resonance, in the 1D model,[20] the linewidth $\Delta$ is related to the damping parameter $\alpha$ by

$$\Delta = \frac{\gamma_0 \alpha H_d}{2\pi}, \qquad (3)$$

where $\gamma_0$ is the gyromagnetic ratio, $\Delta$ the linewidth in Hz, and $H_d$ the demagnetizing field, that we calculate to be equal to 0.45 MA/m in our samples where the magnetization of the free NiFe layer is 0.47 MA/m (see supplementary material[17]). Based on this 1D model (Eq. (3)), the expected linewidth for the DW resonance peak is 0.15 GHz (when $\alpha = 0.01$), in a good agreement with the linewidth extracted from micromagnetic simulations in Fig. 3(a). This result indicates that the 1D model is valid for evaluating the damping extracted from the experimental linewidth measurements for the DW. Regarding mode 2, the linewidth extracted from micromagnetic simulations in Fig. 3(b) is also 0.15 GHz (when $\alpha = 0.01$). This means that the 1D model, originally defined for a DW dynamic, can also be used to predict the linewidth of the domain resonance peak. This indicates that the mode 2 is associated to a confined localised magnetization and not the entire domain. In order to further understand the origins of these two modes, the mode solver from SpinFlow3D[21,22] was used to fully describe the excitation. The result can be seen in the inset in Fig. 3. The mode 2 can be clearly identified as belonging to a localised edge mode in the left foot of the sample (inset in Fig. 3(b)). As to the mode 1, it is identified as a translational vibration mode of the DW (inset in Fig. 3(a)).[21]

The 1D model expression (Eq. (3)) can be used to evaluate the damping associated to the linewidth extracted from the measurements (Fig. 2), which is about $0.4 \pm 0.02$ GHz for the two modes. The corresponding damping $\alpha$ is 0.026 $\pm$ 0.001 both for the DW and the edge mode magnetization oscillations. This value of $\alpha$ is more than twice the value that we have measured by FMR on an unpatterned film ($0.01 \pm 0.0015$) which is more consistent with what is typically observed in Py films ($0.01^{11}$) (see supplementary material[17]). For each of the five samples we have measured, we have obtained similar large damping values for the vibrational modes, in the range 0.019–0.028.

Several mechanisms can be involved in this large increase in the effective damping compared to classical FMR measurements on thin films. We consider possible effects that are present and estimate their relative contributions. One source of increased damping can be due to surface roughnesses or edge defects,[24] but it has been recently shown by micromagnetic simulations that the resulting damping is an order of magnitude smaller than what we observe.[25,26]

Another potential source of increased damping, especially in the case of a DW, has been shown by Ndjaka *et al.*[27] In trilayer structures, the stray field generated by DWs in one ferromagnetic layer dipolarly couples to the other ferromagnetic layer, leading, in the case of very strong coupling, to DW and domain duplication.[28,29] In the case of weak coupling, such as expected in our samples because the SAF prevents domains duplication, only a local perturbation of the magnetization in the reference layer is observed.[27] The magnetic shadow in the reference layer coupled with the DW
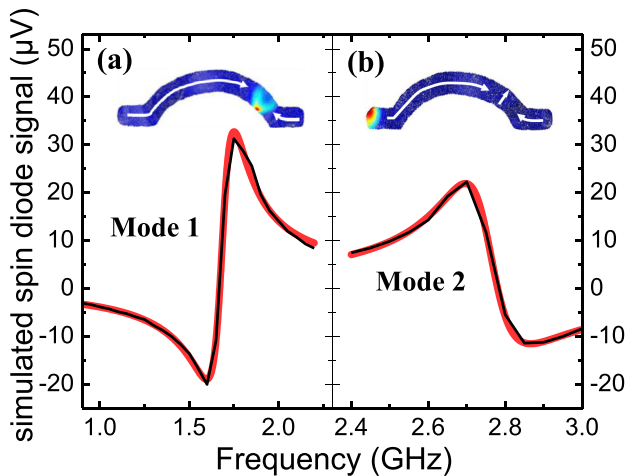


FIG. 3. Spin diode signal reconstructed from micromagnetic simulations of the Py free layer at zero external field. (a) Black line: Reconstructed spin diode signal in the 0.9–2.2 GHz frequency range, showing the resonant response of the DW (mode 1). -Red line: fit with Eq. (2). (b) Black line: Reconstructed spin diode signal in the 2.4–3 GHz frequency range showing the domains resonant response (mode 2). Red line: fit with Eq. (2). Insets: Spatial distribution of the amplitude of the magnetization oscillations dynamic component from the SpinFlow3D mode solver associated with the two observed modes. The color scale blue-green-yellow-red corresponds to the amplitude of the mode. The white arrows show the direction of the magnetization.

dynamic in the upper one results in an increased damping. To confirm and quantify this behavior, we have performed micromagnetic simulations of the full stack, the parameters of which are given in Ref. 23. Figs. 4(a) and 4(b) show, respectively, the magnetization of the Py free layer and the CoFeB reference layer. As expected, we observe that the magnetization of the reference layer reveals a non-uniformity located just below the DW of the free layer. In order to quantify this effect, we extract the effective DW damping, denoted $\alpha_{DW}$, from the DW damped oscillations as a function of $\alpha_{ref}$, the damping of the SAF layers (Fig. 4(c)). In the simulations, we set the damping of the free layer to 0.01, and vary the damping of the SAF layers between 0 and 0.1. Figure 4(c) shows the dependence of $\alpha_{DW}$ on $\alpha_{ref}$ for two values of the Ruderman-Kittel-Kasuya-Yosida (RKKY) interlayer exchange coupling in the SAF: $-1 \times 10^{-4}$ (filled symbols) and $-3 \times 10^{-4}$ (open symbols) J/m$^2$ and for three values of the reference CoFeB layer magnetization: 0.82 MA/m, 1.03 MA/m, and 1.2 MA/m. In each case, we observe an increase of $\alpha_{DW}$ with $\alpha_{ref}$, thus confirming the dynamic coupling between the DW and its magnetic shadow. In our experiments, the typical values of the RKKY exchange coupling, $\alpha_{ref}$ and Ms for the CoFeB reference layer are, respectively, $-0.1$ erg/cm$^2$, 0.01 and 1.2 MA/m.[30,31] As shown in Figure 4(c), the corresponding $\alpha_{DW}$ is about 0.0115, meaning that the DW damping increase due to dipolar coupling is one order of magnitude smaller than what we observe (see supplementary material[17]).

An alternative phenomenon that can lead to strong damping increases is intralayer transverse spin pumping.[25,26,32,33] In a conducting ferromagnet, the conduction electrons carry away the excess angular momentum of a precessing magnetization.

For spatially inhomogeneous magnetization dynamics, a nonuniform spin current is induced, resulting in a spatial dependence of the dissipative flow of conduction electrons in the magnetic layer itself. This can give rise to an enhanced damping in isolated magnetic nanostructures. This intralayer spin current results in the following additional nonlocal torque in the Landau-Lifshitz-Gilbert equation:[26] $\sigma_T$ $(\vec{m} \times \nabla^2 \frac{\partial \vec{m}}{\partial t})$, where $\sigma_T$ is the transverse spin conductivity. In Ref. 32, the increase of damping due to intralayer spin pumping is estimated by $\eta \left( \frac{2\pi}{\lambda} \right)^2$, where $\eta = \frac{g \mu_B \hbar G_0}{4 e^2 M_S}$, is a material dependent parameter related to $\sigma_T$ of Ref. 26. The parameter $\lambda$ is the wavelength for the magnetization pattern we consider. This means that the more magnetization dynamics are spatially confined and smaller the resulting $\lambda$, and the more the increase of damping is important. The spatial profile of the calculated modes shown in the inset of Fig. 3 can give us a rough estimate for $\lambda$, typically 100 nm for both DW and edge modes. By taking the parameter $\eta$ equal to 0.76 nm$^2$ for Permalloy with $M_S = 0.47$ MA/m and the conductivity $G_0 = (5 \, \mu\Omega \, cm)^{-1}$,[32] we find that the associated damping increase is 0.003. Recent analytical calculations confirm that for transverse domain walls damping increases due to intralayer spin pumping are very small.[34]

In our experiments, the injected microwave current density is 1.43 $10^5$ A/cm$^2$, about 10 times smaller than the critical current densities needed to depin the domain wall.[16] From the measured rectified voltages in Fig. 2, we find that the amplitude of domain wall translation at resonance is 4 nm, non-negligible compared to the domain wall width of 100 nm. It has been shown experimentally that non-linear contributions, which are not accounted for in micromagnetic simulations, can give rise to very large damping increases in nanostructures.[35] By a process of elimination, it seems that only these non-linear contributions, appearing for wide vibration amplitudes, can be responsible for the very large damping values that we measure. Our results are in agreement with the high damping values generally derived from magnetic field or spin torque driven domain wall motion over large distances.[36] They also show that the damping of simple objects like a transverse domain wall in a standard material such as Permalloy is still far from being understood.

In conclusion, we have shown that by combining the spin diode effect with the large magneto-resistance ratios provided by magnetic tunnel junctions, we can quantitatively analyze the resonance of individual magnetic confined modes. The effective damping of the domain wall and edge mode extracted from the rectified spin diode signal is more than double compared to that extracted from the FMR measurements on the extended stack. We ascribe our observations to non-linear contributions to the damping due to the large amplitudes of vibration. Our results underline that damping mechanisms are still far from being understood in simple magnetic systems. They also show that non-linear contributions should be taken into account when modeling large amplitude vibrations or translations of solitons in magnetic nanostructures, in particular, for memory and logic applications.
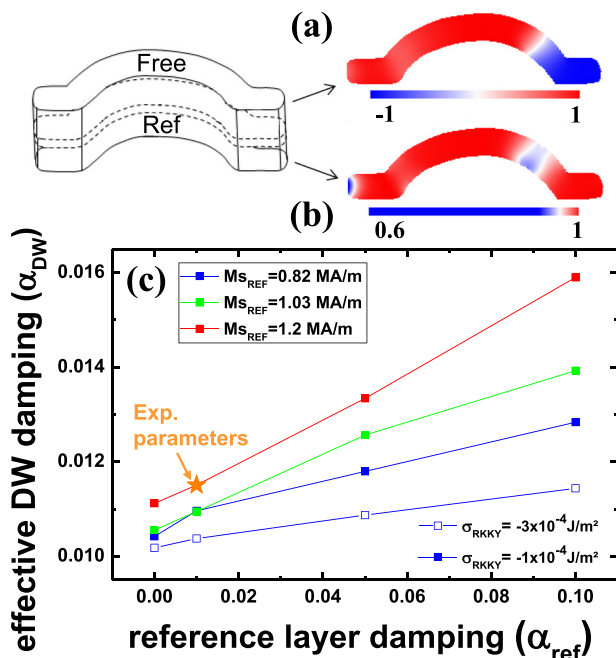


FIG. 4. OOMMF micromagnetic simulations of the Permalloy free layer with the DW (a) and the CoFeB reference layer (b). (c) Dependence of the DW effective damping on the reference layers damping. The filled (resp. open) symbols correspond to an RKKY exchange coupling in the SAF of $-1.10^{-4}$ J/m$^2$ (resp. $-3.10^{-4}$ J/m$^2$). The value of the CoFeB reference layer magnetization is varied between 0.82 MA/m, 1.03 MA/m, and 1.2 MA/m.

external field value, as well as the VNA FMR measurements of an unpatterned film used to extract the damping of the Py free layer. The last part shows the details of the micromagnetic simulations performed on the full stack in order to quantify the dipolar coupling between the DW and the reference layer as a function of $\alpha_{ref}$.

[1]A. A. Tulapurkar, Y. Suzuki, A. Fukushima, H. Kubota, H. Maehara, K. Tsunekawa, D. D. Djayaprawira, N. Watanabe, and S. Yuasa, Nature **438**, 339 (2005).

[2]D. Bedau, M. Klaui, S. Krzyk, U. Rudiger, G. Faini, and L. Vila, Phys. Rev. Lett. **99**, 146601 (2007).

[3]D. Bedau, M. Klaui, M. T. Hua, S. Krzyk, U. Rudiger, G. Faini, and L. Vila, Phys. Rev. Lett. **101**, 256602 (2008).

[4]J.-S. Kim, O. Boulle, S. Verstoep, L. Heyne, J. Rhensius, M. Klaui, L. J. Heyderman, F. Kronast, R. Mattheis, C. Ulysse, and G. Faini, Phys. Rev. B **82**, 104427 (2010).

[5]C. T. Boone, J. A. Katine, M. Carey, J. R. Childress, X. Cheng, and I. N. Krivorotov, Phys. Rev. Lett. **104**, 097203 (2010).

[6]J. Grollier, M. V. Costache, C. H. van der Wal, and B. J. van Wees, J. Appl. Phys. **100**, 024316 (2006).

[7]P. Metaxas, A. Anane, V. Cros, J. Grollier, C. Deranlot, Y. Lemaitre, S. Xavier, C. Ulysse, G. Faini, F. Petroff, and A. Fert, Appl. Phys. Lett. **97**, 182506 (2010).

[8]A. S. Jenkins, E. Grimaldi, P. Bortolotti, R. Lebrun, H. Kubota, K. Yakushiji, A. Fukushima, G. de Loubens, O. Klein, S. Yuasa, and V. Cros, Appl. Phys. Lett. **105**, 172403 (2014).

[9]A. S. Jenkins, R. Lebrun, E. Grimaldi, S. Tsunegi, P. Bortolotti, H. Kubota, K. Yakushiji, A. Fukushima, G. De Loubens, O. Klein, S. Yuasa, and V. Cros, e-print arXiv:1505.05358.

[10]J. C. Sankey, P. M. Braganca, A. G. F. Garcia, I. N. Krivorotov, R. A. Buhrman, and D. C. Ralph, Phys. Rev. Lett. **96**, 227601 (2006).

[11]G. D. Fuchs, J. C. Sankey, V. S. Pribiag, L. Qian, P. M. Braganca, A. G. F. Garcia, E. M. Ryan, Z.-P. Li, O. Ozatay, D. C. Ralph, and R. A. Buhrman, Appl. Phys. Lett. **91**, 062507 (2007).

[12]C. Wang, Y.-T. Cui, J. Z. Sun, J. A. Katine, R. A. Buhrman, and D. C. Ralph, J. Appl. Phys. **106**, 053905 (2009).

[13]S. Ishibashi, T. Seki, T. Nozaki, H. Kubota, S. Yakata, A. Fukushima, S. Yuasa, H. Maehara, K. Tsunekawa, D. D. Djayaprawira, and Y. Suzuki, Appl. Phys. Express **3**, 073001 (2010).

[14]R. Matsumoto, A. Chanthbouala, J. Grollier, V. Cros, A. Fert, K. Nishimura, Y. Nagamine, H. Maehara, K. Tsunekawa, A. Fukushima, and S. Yuasa, Appl. Phys. Express **4**, 063001 (2011).

[15]M. J. Donahue and D. G. Porter, Interagency Report No. NISTIR 6376, National Institute of Standards and Technology, Gaithersburg, MD, 1999.

[16]J. Sampaio, S. Lequeux, P. J. Metaxas, A. Chanthbouala, R. Matsumoto, K. Yakushiji, H. Kubota, A. Fukushima, S. Yuasa, K. Nishimura, Y. Nagamine, H. Maehara, K. Tsunekawa, V. Cros, and J. Grollier, Appl. Phys. Lett. **103**, 242415 (2013).

[17]See supplementary material at http://dx.doi.org/10.1063/1.4935203 for the description of the experimental set-up and for the full demonstration of Eq. (2). The measurements of the rectified voltage are shown for all the

[18]C. Wang, Y.-T. Cui, J. Z. Sun, J. A. Katine, R. A. Buhrman, and D. C. Ralph, Phys. Rev. B **79**, 224416 (2009).

[19]The 5 nm Py free layer is considered with a cell size of 4.4 nm $\times$ 4.4 nm $\times$ 5 nm (where the shape corresponds to the SEM image of Fig. 1). The magnetic parameters are: Ms = 0.47 MA/m, $\alpha$ = 0.01, and A = 13 pJ/m and the spin transfer torque parameters are the current polarization of 0.3 and field-like to Slonczewski torque ratio of 0.1.

[20]A. Thiaville and Y. Nakatani, "Spin dynamics in confined magnetic structures III," Top. Appl. Phys. **101**, 161–206 (2006).

[21]P. J. Metaxas, M. Albert, S. Lequeux, V. Cros, J. Grollier, A. Anane, and H. Fangohr, e-print arXiv:1411.4502.

[22]V. V. Naletov, G. de Loubens, G. Albuquerque, S. Borlenghi, V. Cros, G. Faini, J. Grollier, H. Hurdequint, N. Locatelli, B. Pigeau, A. N. Slavin, V. S. Tiberkevich, C. Ulysse, T. Valet, and O. Klein, Phys. Rev. B **84**, 224423 (2011).

[23]The full magnetic stack and associated parameters considered for micromagnetic simulations are: CoFe pinned [$M_s$ = 0.69 MA/m] (2.5 nm)/ Ru (1 nm)/CoFeB [$M_s$ = 1 MA/m] (3 nm)/MgO (1 nm)/NiFe free [$M_s$ = 0.47 MA/m] (5 nm).

[24]O. Ozatay, P. G. Gowtham, K. W. Tan, J. C. Read, K. A. Mkhoyan, M. G. Thomas, G. D. Fuchs, P. M. Braganca, E. M. Ryan, K. V. Thadani, J. Silcox, D. C. Ralph, and R. A. Buhrman, Nat. Mater. **7**, 567–573 (2008).

[25]T. Weindler, H. G. Bauer, R. Islinger, B. Boehm, J.-Y. Chauleau, and C. H. Back, Phys. Rev. Lett. **113**, 237204 (2014).

[26]H. T. Nembach, J. M. Shaw, C. T. Boone, and T. J. Silva, Phys. Rev. Lett. **110**, 117201 (2013).

[27]J. M. B. Ndjaka, A. Thiaville, and J. Miltat, J. Appl. Phys. **105**, 023905 (2009).

[28]L. Thomas, J. Luning, A. Scholl, F. Nolting, S. Anders, J. Stohr, and S. S. P. Parkin, Phys. Rev. Lett. **84**, 3462 (2000).

[29]D. Lacour, M. Hehn, O. Lenoble, A. Schuhl, C. Tiusan, and K. Ounadjela, J. Appl. Phys. **89**, 8006 (2001).

[30]T. Devolder, P.-H. Ducrot, J.-P. Adam, I. Barisic, N. Vernier, J.-V. Kim, B. Ockert, and D. Ravelosona, Appl. Phys. Lett. **102**, 022407 (2013).

[31]S. Ikeda, K. Miura, H. Yamamoto, K. Mizunuma, H. D. Gan, M. Endo, S. Kanai, J. Hayakawa, and H. Ohno, Nat. Mater. **9**, 721–724 (2010).

[32]S. Zhang and Steven S.-L. Zhang, Phys. Rev. Lett. **102**, 086601 (2009).

[33]Y. Tserkovnyak, E. M. Hankiewicz, and G. Vignale, Phys. Rev. B **79**, 094415 (2009).

[34]J.-V. Kim, e-print arXiv:1502.04695.

[35]C. T. Boone, J. A. Katine, J. R. Childress, V. Tiberkevich, A. Slavin, J. Zhu, X. Cheng, and I. N. Krivorotov, Phys. Rev. Lett. **103**, 167601 (2009).

[36]O. Boulle, G. Malinowski, and M. Klaeui, Mater. Sci. Eng., R **72**, 159 (2011).